Second International Symposium on Marine Propulsors
smp'11, Hamburg, Germany, June 2011

Exploring the Potential of an Oscillating Duct as a Marine Propulsor

Gerasimos Politis [1], Vasileios Tsarsitalidis [2]

[1]Associate professor, NTUA, Athens Greece
[2]Naval Architect and Marine Engineer, PHD candidate, NTUA Athens, Greece

ABSTRACT

Inspired by the paradigm of a jellyfish or a torpedo fish, where a bulk muscle oscillatory motion produces thrust, we have taken the initiative to explore the propulsion capabilities of a new propulsor concept based on an oscillating/pulsating flexible duct. We term this new propulsor 'Flexible Oscillating Duct' or simply, FOD. To understand the flow physics of the FOD system, the problem of flow around an actively (i.e. controlled by the user) deforming FOD, performing unsteady motion, while travelling with a given velocity in an infinitely extended fluid, is formulated and solved using a nonlinear potential based 3D BEM. Dynamic evolution of unsteady trailing vortex sheets, emanating from the trailing edges of the FOD body, is calculated by applying the kinematic and dynamic boundary conditions as part of a time stepping algorithm used for the solution of the unsteady problem. A nonlinear, pressure-type Kutta condition has been applied at the FOD trailing edge. With the proper filtering of induced velocities, which introduces artificial viscosity to our model, roll-up patterns emerge, indicating the main vortex structures by which the wake interacts with the FOD body to develop forces. For the needs of the simulation, a special data generation algorithm has been developed, capable of producing a number of unsteady motions for the FOD, including chord-wise flexibility. Using this data-generation code, we feed the BEM code with systematic motion data by varying the pitch angle of the FOD sections, as well as the Strouhal number. Systematic results for the open water thrust, power and efficiency are calculated and presented. The problem of designing such a system for a real ship is also presented. Comparisons with a conventional propeller prove that the FOD is a promising system with propulsive coefficients comparable to that of a conventional propeller.

Keywords

Oscillating duct, Jellyfish Propulsion, Biomimetics, Flapping foil propulsion, Boundary element method, Unsteady wake rollup

1 INTRODUCTION

Economic and ecological reasons, scarcity of resources and demand for speed dictate an ever-growing drive for efficiency. The application of biomimetic systems of propulsion is far from new as a thought, yet it is considered immature despite the fact that has been utilized by birds and sea creatures for millions of years. In some of his works, the philosopher Aristotle considers the anatomy and locomotion of swimming creatures. Leonardo Da Vinci had also made many designs of bird-like flying machines, which would be successful had he today's technology.

The modern history of biomimetics starts in 1935 with Gray's paradox, and theoretical developments start with the works of Sir James Lighthill (1969) and T.Y. Wu (1971). A thorough review of those theories can be found in Sparenberg (2002). Thorough reviews of computational and experimental work in biomimetics can be found in the review papers of Shyy et al (2010) regarding aerodynamics and aeroelasticity; of M. Triantafyllou et al (2004) regarding experimental developments; and of Rozhdestvensky (2003) regarding all types of applications, even full scale. Interesting information can also been found in the books by Alexander, Shyy et al and Taylor et al. Marine biomimetic propulsors are also discussed in the book of N. Bose.

The present work is devoted in a preliminary numerical investigation of the feasibility of a FOD to propel a real ship. A natural paradigm of a propulsor with similar thrust production mechanisms to that of the FOD, is the jellyfish. Jellyfish flow mechanics has been investigated by Dabiri (2005, 2006), who has made many numerical and experimental simulations and has shown the feasibility of using variable diameter nozzles as propulsors.

Flow simulations using BEM is a well-developed and successful mathematical/numerical theory with very good predictions for cases where lift is the main mechanism of force production (Katz & Plotkin 2001). The first 3-D BEM for analyzing the flow around arbitrary non-lifting bodies can be attributed to Hess & Smith (1962). The first 3-D BEM for analyzing the steady flow around a marine

propeller can be attributed to Hess & Valarezo (1985). In this paper, the classical Hess & Smith lifting formulation has been used for the representation of a steadily translating and rotating propeller using a prescribed wake shape (PWS) to model trailing vortex sheets. In the following years, various alternative formulations of the panel method have been applied for the solution of flow problems. A brief presentation of the historical aspects of propeller related BEM formulations can be found in Politis (2004). Furthermore, this paper presents the formulation and solution of the problem of an unsteadily moving propeller using a Morino-type BEM. The main innovation in this formalism is the capability of calculation by the code of the evolution of the free vortex sheet emanating from the propeller blades. During the period 2002-2008, this code, initially developed to treat propeller problems, has been expanded to include the 3-D unsteady incompressible non-viscous flow problem around an arbitrary system of interacting non-lifting/lifting rigid/flexible bodies (Politis 2009, 2011). Furthermore, in Politis & Tsarsitalidis (2009), there is a first attempt to systematically investigate the effect of flapping foil propulsor geometry, on its open water performance using this 3D BEM code.

In this paper, a new propulsor concept named FOD is introduced and its hydrodynamic performance is investigated and compared with that of a conventional propeller. The FOD is capable of changing its geometry (diameter, pitch) harmonically with time, in a specific way, similar to that used in 2-D flapping foils, but with an additional oscillation in camber. A data generation program has been developed, producing the FOD panel geometry and motion. The produced time dependent geometry has then been introduced to the BEM code, which solves the hydrodynamic flow problem around the moving/deforming FOD, and calculates the trailing shear layer time-dependent geometry, the developed thrust and the energy demand for the motion of the FOD. Systematic runs have been made for a range of Strouhal numbers and pitch angles at a pre-selected heave to chord ratio. Those results have then been used to undertake powering performance calculations for the FOD propulsor. Powering performance calculations have also been made for the ship equipped with a conventional propeller. The comparison shows that the FOD can produce high efficiencies, thus giving a serious reason for further investigating such a propulsor in order to overcome the technical difficulties connecting with its construction.

2 FOD GEOMETRY AND MOTION – PANEL GENERATION

The starting point for an unsteady BEM simulation of a flexible body is the generation of the time dependent paneling describing the geometry of the system (Politis 2011). The FOD time dependent geometry is produced in the following way:

We start from a conventional 2-D foil moving parallel to the X -axis with velocity U . The foil performs a heaving motion (along the vertical Y -axis) with amplitude h_0 and a pitching motion with amplitude θ_0 and a phase angle ψ with respect to the heaving motion. The pitching motion is performed around a pre-selected given pitching axis. Both heaving and pitching motions are performed with angular velocity $\omega = 2\pi n$, where n is the corresponding frequency. Furthermore, the camber of the 2-D foil performs an unsteady motion with a chord-wise distribution $y_c(t,u)$, taken from the NACA series, with an instantaneous maximum camber $m_c(t)$ (expressed as a fraction of chord). An oscillating camber motion can then be obtained by deciding about the form of the function $m_c(t)$. There are at least three possible reasonable selections for $m_c(t)$: (a) select $m_c(t)$ such that the instantaneous effective (i.e., with respect to the total flow velocity) angle of attack of the section coincides with the ideal angle of attack of the section (i.e., the section operates in its shock free entry at all times), (b) select $m_c(t)$ to oscillate harmonically with the same frequency and phase as that used for the pitching motion, and a maximum value m_0 which results to an ideal angle of attack equal to the effective maximum angle of attack of the flapping foil, and (c) select $m_c(t)$ to oscillate harmonically with the same frequency and phase as that used for the pitching motion, and a maximum predetermined (user defined) value m_0. In this case, part of lift is produced by the camber and part by the additional angle of attack. Notice that in all cases the camber unsteady motion has the same frequency and the same phase with that of the pitching motion. On the other hand, only cases (b) and (c) are pure harmonic motions.

With the previous discussion in mind, at each time t we have defined the foil geometry and position in the aforementioned XY plane. Taking an axis L parallel to the X axis, at a distance R along Y axis and rotating the foil by 360 deg around L, we get the FOD configuration at this time step. We term R the FOD radius and $D = 2 \cdot R$ the FOD diameter.

As a result of the previous discussion, the instantaneous angle of attack $a(t)$ of a section (2-D foil) of the FOD, with respect to the undisturbed flow (resulting from the parallel movement along X-axis and the heaving motion), is given by the equation:

$$a(t) = \theta_0 \sin(2\pi n \cdot t + \psi) - \tan^{-1}\left(\frac{h_0 2\pi n \cdot \cos(2\pi n \cdot t)}{U}\right) \quad (1)$$

or in non-dimensional form:

$$a(t) = \theta_0 \sin(2\pi n \cdot t + \psi) - \tan^{-1}(\pi \cdot St \cdot \cos(2\pi n \cdot t)) \quad (2)$$

where St denotes the Strouhal number defined by:

$$St = \frac{n \cdot h}{U}, h = 2h_0 \quad (3)$$

and h denotes the heave height.

Furthermore, assuming a NACA four digit camber distribution, the camber motion is described by the following equations:

$$y_c(t,u) = m_c(t)\frac{c\cdot u}{p^2}(2p-u), 0 \le u \le p \quad (4)$$

$$y_c(t,u) = m_c(t)\left(\frac{c\cdot(1-u)}{(1-p)^2}\right)\cdot(1+u-2\cdot p), p \le u \le 1 \quad (5)$$

where $m_c(t)$ is the maximum instantaneous camber as a fraction of chord, p is the location of maximum camber (as a fraction of the chord) and u is the non-dimensional chord-wise position (Abbott & Doenhoff 1959).

We are now ready to calculate the time evolution of maximum camber for the cases (a) and (b) discussed previously. For case (a) the instantaneous maximum camber is given by:

$$m_c(t) = \frac{f_{3D}\cdot a(t)\cdot p^2(-p+1)^2\pi}{2(p-\frac{1}{2})(p^2\pi - 2p\vartheta + \vartheta - \sin(\vartheta))} \quad (6)$$
$$\vartheta = a\cos(1-2p)$$

where $a(t)$ is calculated from (2) and f_{3D} is a correction factor for passing from the undisturbed entrance to the effective entrance (estimated heuristically). For case (b) the instantaneous maximum camber is given by:

$$m_c(t) = m_0\sin(2\pi n\cdot t + \psi) \quad (7)$$

where:

$$m_0 = \frac{f_{3D}\cdot a_{\max}\cdot p^2(-p+1)^2\pi}{2(p-\frac{1}{2})(p^2\pi - 2p\vartheta + \vartheta - \sin(\vartheta))} \quad (8)$$
$a_{\max} = \max_{t\in(0,T)}(a(t))$, T denotes the motion period

Finally for case (c), equation (7) is applied, with m_0 heuristically selected by the designer.

Relations (8) are produced by applying the formula for the ideal angle of attack to the camber line(4), (5) (Abbott & Doenhoff 1959).

Having introduced the analytical description of both geometry and motion of our FOD, we can now proceed to the creation of a surface panel distribution describing the FOD at consecutive time steps.

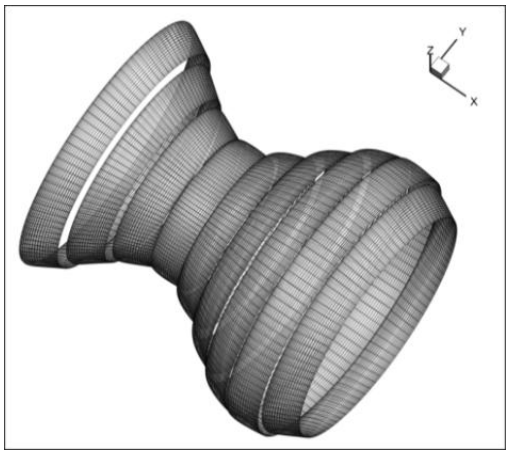

Figure 1: Panel discretization at selected time steps

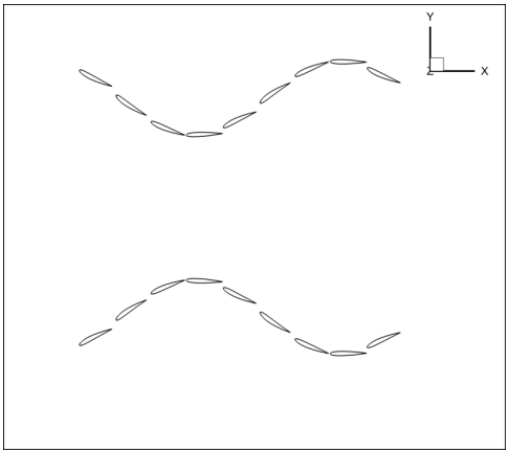

Figure 2: Section of the FOD at selected time steps

Figure 1 shows the panel discretization of the FOD at nine time instances, corresponding to the maximum, minimum and inflection point positions of a FOD section in one period. Figure 2 shows the section of the FOD with a plane containing the X axis for the same time instances.

With the FOD paneling in time known, the unsteady BEM code (Politis 2011) can be applied to calculate the FOD unsteady forces, energy requirements and free shear layer evolution.

3 CALCULATION OF FORCES, MOMENTS, POWER AND EFFICIENCY

In the case of a flexible body, energy is transferred through flexibility in a point-wise manner. To overcome this difficulty, the unsteady BEM code uses a specialized procedure for the calculation of the power provided to the FOD mechanism, termed DHP (Delivered Horse Power) and the power developed by the FOD to propel the ship, termed EHP (Effective Horse Power). The corresponding methodology has already been explained in Politis & Tsarsitalidis (2009) and will be repeated here for completeness.

Let A a point belonging to the surface S of a body of our system. Let $\vec{F}$ denote the total force exerted by the fluid to the body at A. This force is a sum of pressure forces normal to body denoted by $\vec{P}$ and viscous forces tangential to body denoted by $\vec{D}$. Thus:

$$\vec{F} = \vec{P} + \vec{D} \quad (9)$$

Let also $\vec{v}$ denote the velocity of A with respect to an inertia reference frame. Consider also a parallel vector field $\vec{d}$ with $\vec{d}$ a unit vector. Then:

$$\vec{v} = (\vec{d}\cdot\vec{v})\cdot\vec{d} + (\vec{d}\times\vec{v})\times\vec{d} \quad (10)$$

The power done from the fluid to the body at A is given by:

$$pow = \vec{F}\cdot\vec{v} = (\vec{F}\cdot\vec{d})(\vec{d}\cdot\vec{v}) + \vec{F}\cdot((\vec{d}\times\vec{v})\times\vec{d}) \quad (11)$$

and the net power from a system of flexible bodies is given by:

$$net\_pow = \int_S \vec{F}\cdot\vec{v}\cdot dS = \int_S (\vec{F}\cdot\vec{d})(\vec{d}\cdot\vec{v})\cdot dS + \int_S \vec{F}\cdot((\vec{d}\times\vec{v})\times\vec{d})\cdot dS \quad (12)$$

In propulsion problems there is always a preferable instantaneous direction in which the system moves. For the FOD case, this is the X axis direction. Take $\vec{d}$ along this direction. Then the first term in the rhs of equation (12) is the instantaneous EHP and the second term is the instantaneous DHP. The ratio EHP/DHP defines the instantaneous efficiency. For the application of the previous formulas the pressure forces on element centroids can be calculated from the unsteady Bernoulli equation (Politis 2011). The code also contains a simple subroutine for the calculation of viscous forces using an elemental surface drag coefficient, which depends on the local Reynolds number with a drag correction for an estimated sectional angle of attack greater that the ideal.

4 FORMULATION AND SOLUTION OF THE FOD PROPULSOR DESIGN PROBLEM

FOD Propulsor design problem consists in finding the propulsor geometric and motion characteristics by which it can propel a given ship with a given ship speed. Although the optimum propulsor problem is a problem of mutual propulsor/stern optimization, in most cases we optimize the propulsor assuming the hull/stern geometry is given.

Development of a design theory for a new propulsor, requires decisions regarding the independent geometric/motion variables controlling the thrust production and the energy absorption. Fortunately, the proposed FOD system is a generalization of the well-developed flapping wing. Thus, the corresponding decisions are straight-forward as follows:

Independent variables by which the state of the FOD is defined uniquely can be decomposed in two groups. *Group A* contains the geometric variables and *Group B* contains the motion related variables.

Group A: Assuming geometrical similarity, a minimum set of parameters defining flexible vibrating duct propulsor geometry is the section chord c, the chord-wise position of the pitching axis b, the duct mean radius R (defined at the position of sectional pitching axis) or equivalently the duct mean diameter D. In non-dimensional form, FOD geometry is characterized by: $(h_0/c, R/c, b/c)$ Notice that we have intentionally declined to introduce the foil section geometry (thickness and camber forms) as a main geometric parameter of the FOD since it mainly controls phenomena like viscous pressure drag, as well as separation at larger angles of attack, and not the FOD thrust and power (i.e., exerts a secondary effect on thrust and power).

Group B: FOD motion is defined by: (i) the amplitude h_0 of a sinusoidal heaving motion of each section normal to the velocity of advance U, (ii) the amplitude θ_0 of a sinusoidal pitching motion, (iii) the amplitude $m_c(t)$ of the camber deformation, (iv) the frequency n (common to both heaving, pitching motions and camber deformations), and (v) the phase angle ψ between heaving and pitching/camber motions. Assuming that the camber deformation has been selected as in (a) or (b) (Section 1), the motion of FOD is completely defined by the following dimensional variables: $(U, h_0, \theta_0, n, \psi)$. In case camber has been selected as in (c) (Section 1), the motion of FOD is defined by: $(U, h_0, \theta_0, m_0, n, \psi)$. We omit in the sequel the m_0 for the sake of simpler formalism, introducing it only when needed. Using dimensional analysis, the non-dimensional parameters controlling FOD performance can be obtained: (θ_0, St, ψ). Assuming further that $\psi = 90$ deg, we finally arrive at two non-dimensional motion parameters controlling the FOD motion: (θ_0, St)

Recapitulating the discussion under (A) and (B), the FOD performance is controlled by the following geometric and motion parameters: $(\theta_0, St, h_0/c, R/c, b/c)$. Notice that the following conceptual coupling between non-dimensional parameters used in the FOD and the conventional propeller can been made (P/D denotes the propeller pitch ratio, A_E/A_0 denotes propeller blade area ratio, D under the <propeller> column denotes propeller diameter, $c_{0.7R}$ denotes blade chord at 70% of propeller radius):

$$\begin{bmatrix} FOD & \text{Pr}opeller \\ & \frac{P}{D} \\ \theta_0 & \\ \frac{c}{R} & \frac{c_{0.7R}}{D} \\ \frac{h_0}{R} & \frac{A_E}{A_0} \end{bmatrix} \quad (13)$$

A well-posed propulsion problem for a FOD propulsor can be set as follows:

Calculate the instantaneous open water FOD performance using the BEM code for a range of the parameters (θ_0, St) assuming given $(h_0/c, R/c, b/c)$. Calculate then the period-mean values for thrust and delivered power and denote them by: T and DHP respectively. FOD performance can then be expressed by the following non-dimensional thrust and (delivered) power coefficients:

$$C_T = \frac{T}{0.5\rho U^2 S} = C_T(\theta_0, St, R/c, h_0/c, b/c) \quad (14)$$

$$C_P = \frac{DHP}{0.5\rho U^3 S} = C_P(\theta_0, St, R/c, h_0/c, b/c) \quad (15)$$

where S denotes the mean FOD disc surface ($=\pi\cdot R^2$). In self-propulsion conditions, we assume that a Taylor wake fraction w is defined by:

$$U = V(1-w) \quad (16)$$

where V is the ship speed. Furthermore a relative rotative efficiency η_R is defined by:

$$\eta_R = \frac{DHP}{DHP_B} \quad (17)$$

where DHP_B denotes the (period-mean) power delivered to the FOD in self-propulsion conditions. Assuming further that a 'thrust equalization method' has been used for the estimation of FOD-hull interaction coefficients w,t,η_R (where t denotes the thrust deduction factor), the FOD thrust and power, in the self-propulsion conditions becomes:

$$T_B = T = 0.5\rho(V(1-w))^2 S \cdot C_T(\theta_0, \frac{n\cdot 2h_0}{V(1-w)}, \frac{R}{c}, \frac{h_0}{c}, \frac{b}{c}) \quad (18)$$

$$DHP_B\eta_R = 0.5\rho(V(1-w))^3 S \cdot C_P(\theta_0, \frac{n\cdot 2h_0}{V(1-w)}, \frac{R}{c}, \frac{h_0}{c}, \frac{b}{c}) \quad (19)$$

For a self-propelled hull, moving with velocity V, the surrounding fluid interacts with the hull developing a resistance force: $R_0(V)/(1-t)$, where $R_0(V)$ denotes the hull towing resistance. A hull can also pull an object with a force F (case of a tug-boat or a trawler). Then the FOD thrust, under self-propulsion conditions, is given by:

$$T_B = \frac{R_0(V)}{1-t} + F \quad (20)$$

Assuming that $V,\theta_0,c,R,h_0,b,w,t,\eta_R$ are known parameters, Equations (18), (19) and (20) become a non-linear system of three equations with three unknowns: (T, DHP_B, n). This system can be solved for a range of ship speeds: $V \in (V_1, V_2)$ and $\theta_0 \in (\theta_{0-a}, \theta_{0-b})$. We thus obtain the totality of design solutions for the given ship:

$$DHP_B, n \leftarrow V, \theta_0\big|_{given:\ \text{ship, c,R,h}_0\text{,}w,t,\eta_R} \quad (21)$$

The content of Equation (21) can be represented in a 2-D $DHP-n$ diagram in the form of parametric curves of constant V and constant θ_0. Notice that this presentation is similar to that used in conventional propellers, where the propeller pitch ratio P/D is taking the place of θ_0. Using this representation, we can finally extract the required optimum FOD by selecting the characteristics (geometric and motion) which require the minimum DHP for the given ship speed V.

5 WAKE VISUALIZATIONS

The case of a FOD with a NACA 4412 section with time dependent maximum camber according to (c) (i.e., $m_o = 0.04$ in relation (7)) and $R/c = 3$, $h_0/c = 1.0$ (where R is the mean FOD radius measured at the position of pitching axis i.e. 1/3 chord from leading edge) was systematically simulated. Wake visualizations for $Str = 0.3, a_{\max} = 15\text{deg}$ are presented in Figures 3, 4, 5 and 6. More specifically, Figure 3 presents the shear layer during the expansion phase of the FOD motion (diameter increases). Figure 4 presents the shear layer during the contraction phase of the FOD motion. Figure 5 shows a slice of the shear layer of a FOD at Z=0 during the expansion phase.

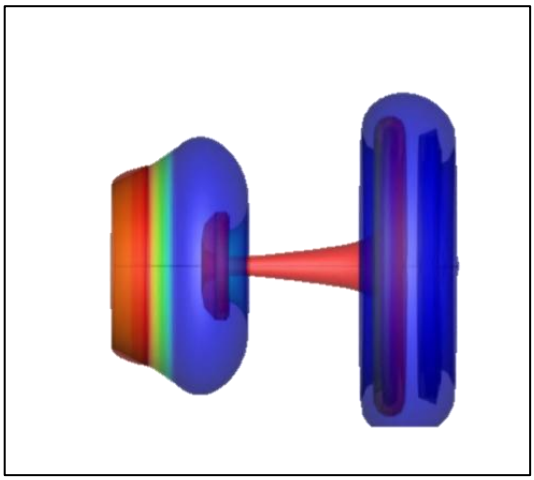

Figure 3: Shear layer of a FOD; instance with duct decreasing diameter

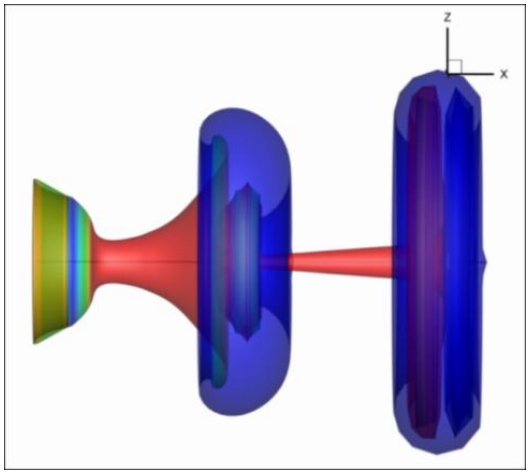

Figure 4: Shear layer of a FOD; instance with duct increasing diameter

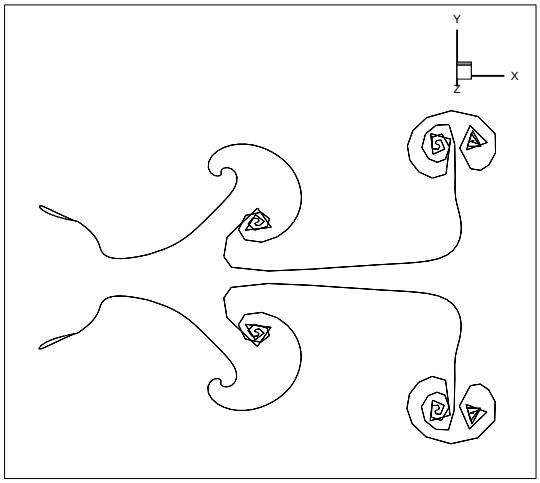

Figure 5: Slice of the shear layer of a FOD at Z=0 showing vortex rollup

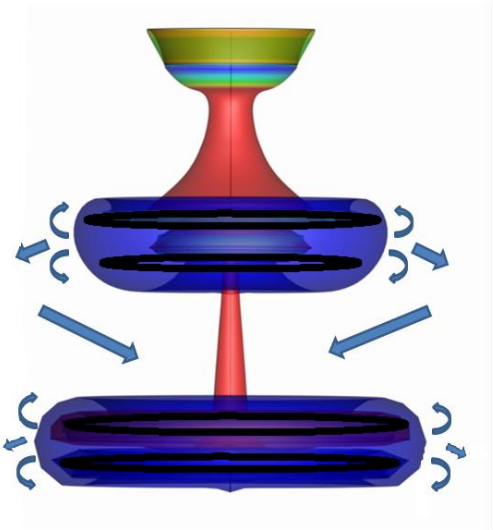

Figure 6: Using wake pattern for vortex structure recognition

Finally, Figure 6 shows the one period wake pattern. The wake pattern deformation acts as a visualizer of the main vortical structure of the wake. This allows us to add some artistic add-ons to the figure, to emphasize this vortical structure. More specifically, the added black circles represent principal vortex rings. Twisted arrows represent the spin direction of the rings and straight arrows the velocities induced by the vortex structure. From Figure 6 it is clearly shown that the FOD, with the exception of the starting ring (where the two ring vortices mutually cancel out), produces a series of oblique jets by which it produces thrust.

6 THE OPEN WATER PERFORMANCE DIAGRAM FOR A FOD WITH GIVEN GEOMETRY

As a design paradigm we have performed systematic open water performance calculations for a FOD with given: $R/c=3$, $h_0/c=1.0, b/c=1/3, c=0.1m$, $Str=0.1\div 0.7$. The presented results have been calculated by running the BEM code for two time periods and calculating the mean values of the unsteady forces over the second period. The base camber distribution for the FOD is the NACA 44. The results are presented in the form of $C_T-\theta_0, C_P-\theta_0$ (where $\theta_0 \rightarrow theta$ in Figures 7 and 8) with parameter the Strouhal number (solid line in the diagrams). Furthermore, Figure 7 contains in a parameteric form (hair lines) the open water efficiency η of the FOD:

$$\eta=\frac{T\cdot U}{DHP}=\frac{C_T}{C_P} \qquad (22)$$

Also, Figure 8 contains in a parametric form the $a_{\max}$ angle (dashed lines) defined as the maximum value of $a(t)$, relation (2), over one period.

Figures 7 and 8 can be used to select an optimum FOD for a given ship using a hand calculator. For example, assume that a ship is given with a design speed of V knots. We would like to design a FOD (i.e., select its optimum geometry with the corresponding revolutions and required DHP). This problem can be solved as follows: (a) with the design speed known, the ship resistance and, from equation (20), the propeller thrust and C_T can be calculated; (b) with this C_T draw a horizontal line on Figure 7 and find the intersection of this horizontal line with the various constant Strouhal lines, let $(\theta_0, St)_i, i=1, n_{str}$ denote the n_{str} intersection points; (c) from each Strouhal number the frequency of the propulsor motion can be found: $n=St\cdot V/(2\cdot h_0)$; (d) use Figure 8 to find C_P for the points $(\theta_0, St)_i, i=1, n_{str}$, from the C_P find the required open water power and use (17) to find DHP_B; (e) from the calculated $DHP_{B,i}, i=1, n_{str}$ select that with minimum required DHP_B.

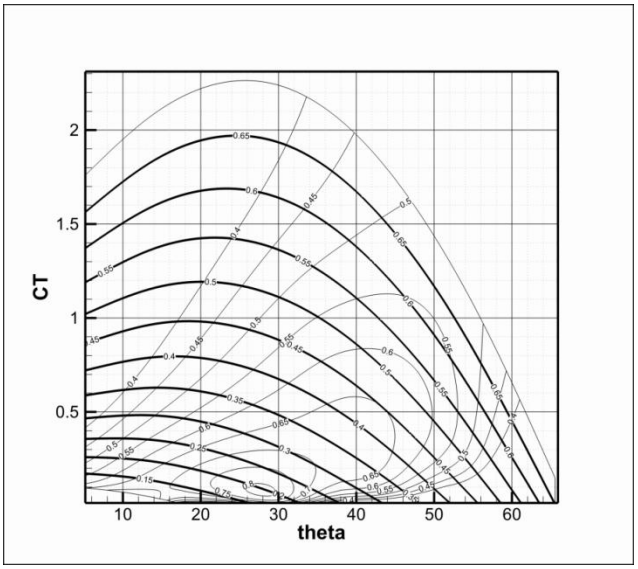

Figure 7: Mean thrust coefficient as a function of θ_0

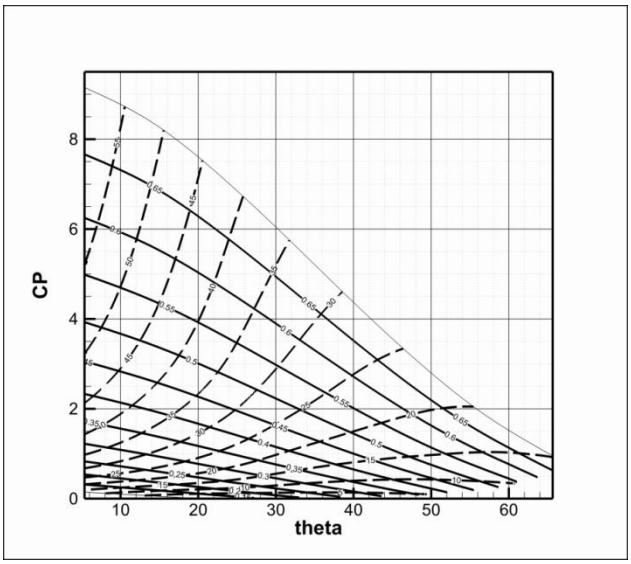

Figure 8: Mean power coefficient as a function of θ_0

7 APPLICATION OF A FOD FOR THE PROPULSION OF A SHIP – OPTIMUM DESIGN EXAMPLE AND COMPARISON WITH CONVENTIONAL PROPELLERS

A high-speed twin screw vessel is used in a feasibility study for the application of a FOD as an alternative propulsor to traditional propellers. The ship bare hull resistance data was taken from the database of the NTUA towing tank and shown in Table 1. With the bare hull resistance given, the system of Equations (18), (19) and (20) can be solved for a range of ship speed V and θ_0 and the totality of design solutions can be presented in a diagram as dictated by Equation (21). For the need of the comparison, we have assumed that in both cases: $w=0.0, t=0.0, \eta_R=1.0$. This is a reasonable assumption since interaction coefficients are (for the same stern geometry) mainly functions of propulsor diameter and developed thrust. Additionally, the vessel in hand is a high speed twin screw which has very small propeller-hull interactions. Also notice that no inclined axis corrections were made for the conventional propellers. Furthermore, no correction of the bare hull resistance (Table 1) for appendages has been made. A shaft efficiency equal to 1 has been used in the calculations.

V (m/s)	R(kp)
10.27	10471
11.32	11519
11.83	11962
12.35	12367
12.87	12697
13.38	13084
13.88	13477
14.40	13872
14.92	14306

Table 1: Bare hull resistance curve for the ship used in the comparative design

The totality of design solutions DHP-N (optimum and non-optimum) for the high speed ship equipped with FODs can be found in Figure 9. Similarly, the totality of design solutions DHP-N (optimum and non-optimum) for the high speed ship, equipped with conventional propellers, can be found in Figure 10. Shown on the figures are the constant-velocity curves and the constant maximum pitch angle θ_0 curves (Fig. 9) or the constant P/D curves (Fig. 10). For a given design speed, the optimum FOD geometry (i.e., θ_0), the corresponding (optimum) FOD frequency (in revolutions per second) and corresponding DHP can be found from Figure 9. Similarly, the optimum propeller geometry (i.e., P/D), the corresponding (optimum) revolutions and the corresponding DHP can be found in Figure 10.

For example, by selecting a ship speed of 28 knots, the optimum FOD propulsor has $\theta_0 = 27\,\text{deg}$ with optimum frequency of nearly 250rpm and required power of 1700 PS, with a propulsive efficiency of 0.78. The optimum B5.70 propeller for the same speed has an optimum P/D=1.4 (although, as Figure 10 indicates, greater P/D can result in better efficiencies) at 345.6 rpm with corresponding required power of 1774.9PS and propulsive efficiency of 0.75.

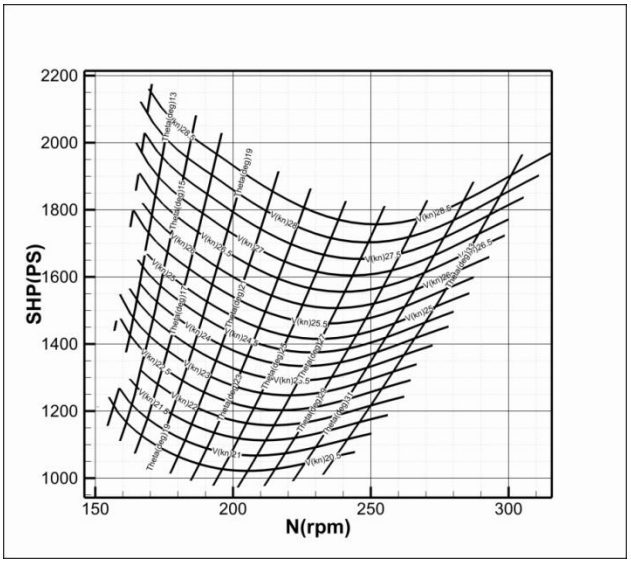

Figure 9: Powering performance of the high speed ship equipped with two FOD propulsors, D=2.3m

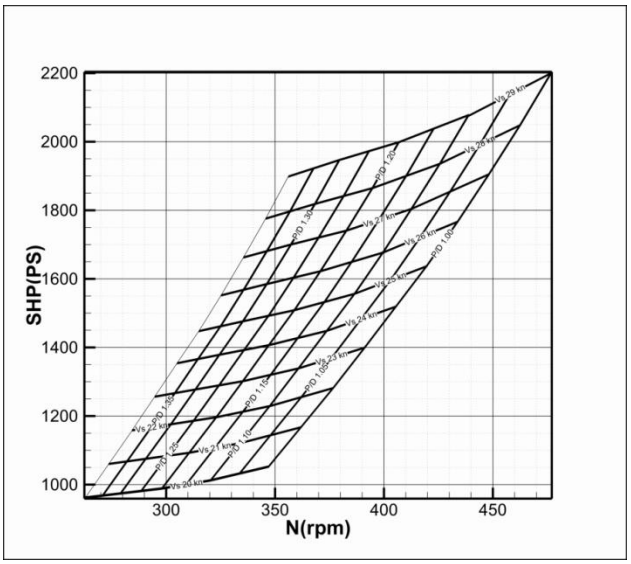

Figure 10: Powering performance of the high speed ship equipped with two B5-70 propellers, D=2m

8 CLOSING REMARKS

We have applied a 3-D BEM time stepping algorithm to investigate the open water performance of a new propulsor concept, the Flexible Oscillating Duct, inspired from the propulsion mechanisms used by squibs and jellyfishes. Our calculations show that the FOD is an efficient propulsor. Propulsive coefficients of the order of

0.78 have been calculated, which are higher than that observed in conventional propellers. It should be noted that the FOD geometry for the needs of this work was randomly selected, since no previous experience/data (either experimental or theoretical) exists. In the near future, we plan to perform systematic open water performance calculations with varying geometric FOD particulars in order to investigate the effect of FOD geometry in its powering characteristics. Obviously, our preliminary analytical calculations indicate that this novel propulsion concept is worth being further examined in all of its aspects.

REFERENCES

Abbott I. & Doenhoff, H. (1959). Theory of Wing Sections. Dover.

Alexander, D. E. Nature's Flyers: Birds, Insects, and the Biomechanics of Flight.

Anderson, J. M., Streitlien, K., Barrett, D. S. & Triantafyllou, M. S. (1998). 'Oscillating foils of high propulsive efficiency'. J. of Fluid Mechanics **360**, pp. 41-72.

Anderson, E. J, & DeMont, M. E. (2000). 'The mechanics of locomotion in the squid Loligo pealei: locomotory function and unsteady hydrodynamics of the jet and intramantle pressure'. J. Exp. Biol. **203**, pp. 2851–63.

Anderson, E. J., & Grosenbaugh, M. A. (2005). 'Jet flow in steadily swimming adult squid'. J. Exp. Biol. **208**, pp. 1125–46.

Aono, H., Liang, F. & Liu, H. (2008). 'Near- and far-field aerodynamics in insect hovering flight: an integrated computational study'. J. Exp. Biol. **211**, pp. 239–57.

Auerbach, D. (1991). 'Stirring properties of vortex rings'. Phys. Fluids **A**(3), pp. 1351–55.

Barrett, D. S. & Triantafyllou, M. S. (1999) 'Drag reduction in fish-like locomotion'. J. of Fluid Mechanics **392**, pp. 183-212.

Beal, D. N. (2003). Propulsion through wake synchronization using a flapping foil., PhD Thesis, MIT.

Borazjani, I. & Sotiropoulos, F. (2008). 'Numerical investigation of the hydrodynamics of carangiform swimming in the transitional and inertial flow regimes'. J. of Exp. Bio. **211**, pp. 1541-1558.

Buchholz, J. H. & Smits, A. J. (2008). 'The wake structure and thrust performance of a rigid low-aspect-ratio pitching panel'. J. of Fluid Mechanics **603**, pp. 331–365.

Czarnowski, J. T. (1997). Exploring the possibility of placing traditional marine vessels under oscillating foil propulsion. Msc Thesis, MIT.

Dabiri, J. O. (2005). 'On the estimation of swimming and flying forces from wake measurements'. J. Exp. Biol. **208**, pp. 3519–32.

Dabiri, J. O. & Gharib, M. (2005a). 'Starting flow through nozzles with temporally variable exit diameter'. J. of Fluid Mechanics **538**, pp. 111–36.

Dabiri, J. O. & Gharib, M. (2005b). 'The role of optimal vortex formation in biological fluid transport'. Proc. R. Soc., **B 272**, pp. 1557–60.

Dabiri, J. O., Colin, S. P. & Costello, J. H. (2006). 'Fast-swimming hydromedusae exploit velar kinematics to form an optimal vortex wake'. J. Exp. Biol. **209**, pp. 2025–33.

Dong, H., Mittal, R. & Najjar, F. M. (2006). 'Wake topology and hydrodynamic performance of low-aspect-ratio flapping foils'. J. of Fluid Mechanics **566**, pp. 309–43.

Ellenrieder, von K. D., Parker, K. & Soria, J. (2003). 'Flow structures behind a heaving and pitching finite-span wing'. J. of Fluid Mechanics **490**, pp. 129–138.

Ellenrieder, von K. D., Parker, K. & Soria, J. (2008). 'Fluid mechanics of flapping wings'. Experimental Thermal and Fluid Science **32**, pp 1578–1589.

Floc'h, F., Laurens, J. M. & Leroux, J. B. (2009). 'Comparison of hydrodynamics performances of a porpoising foil and a propeller'. First International Symposium on Marine Propulsors smp'09, Trondheim, Norway.

Gopalkrishnan, R., Triantafyllou, M. S., Triantafyllou, G. S. & Barrett, D. (1994). 'Active vorticity control in a shear flow using a flapping foil'. J. of Fluid Mechanics **274**, pp. 1-21.

He, M., Veitcha, B., Bose, N., Colbourne, B. & Liu, P. (2006). 'A three-dimensional wake impingement model and applications on tandem oscillating foils'. Ocean Engineering **34**, pp. 1197-1210.

Hess, J. L. & Smith, A. M. O. (1962). 'Calculation of Non-lifting potential flow about arbitrary 3-D bodies'. Douglas Aircraft, Report E.S. 40622.

Hess, J. L. & Valarezo, W. O. (1985). 'Calculation of steady flow around propellers by means of a surface panel method'. 23rd Aerospace Sciences Meeting, AIAA, Reno, Nevada.

Hess, J. L. (1972). 'Calculation of potential flow around arbitrary three dimensional lifting bodies'. McDonnell Douglas Corporation Report MDC J5679-01.

Hover, F. S., Haugsdal, O. & Triantafyllou M. S. (2004). 'Effect of angle of attack profiles in flapping foil propulsion'. J. Fluids Struct. **19**, pp. 37-47.

Katz, J. & Plotkin, A. (2001). Low-Speed Aerodynamics. 2nd ed. Cambridge University Press, New York.

Krylov, V. V. & Porteous, E. (2010). 'Wave-like aquatic propulsion of mono-hull marine vessels'. Ocean Engineering **37**, pp. 378–386.

Licht, S., Hover, F. & Triantafyllou, M. S. (2004). 'Design of a Flapping Foil Underwater Vehicle'. IEEE J. of Oceanic Engineering **21**(3).

Lighthill, M. J. (1969). 'Hydromechanics of aquatic propulsion: a survey'. Annual Review of Fluid Mechanics **1**, pp. 413–446.

Liu, P. & Bose, N. (1997). 'Propulsive Performance from oscilating propulsors with spanwise flexibility'. Proc. R. Soc. Lond. **A**(453), pp. 1763-1770.

Liu, P. & Bose, N. (1999). 'Hydrodynamic characteristics of a lunate shape oscillating propulsor'. Ocean Engineering **26**, pp. 519-529.

Politis, G. K. & Belibasakis, K. A., (1999). 'High propulsive efficiency by a system of oscillating wing tails'. CMEM, WIT Conference.

Politis G. K. (2004). 'Simulation of Unsteady motion of a Propeller in a fluid including Free Wake Modeling'. Journal of Engineering Analysis with Boundary Elements **28**(6), pp. 633-653.

Politis, G. K. (2005). 'Unsteady Rollup modeling for wake adapted propellers Using a time stepping method'. Journal of Ship Research **49**(3).

Politis, G. K. & Tsarsitalidis, V. T (2009). 'Simulating Biomimetic (Flapping Foil) Flows for Comprehension, Reverse Engineering and Design'. First International Symposium on Marine Propulsors smp'09, Trondheim, Norway.

Politis, G. K. (2009). 'A BEM code for the calculation of flow around systems of independently moving bodies including free shear layer dynamics'. Advances in boundary element techniques X, WIT Conference, Athens, Greece.

Politis, G. K. (2011). 'Application of a BEM time stepping algorithm in understanding complex unsteady propulsion hydrodynamic phenomena'. Ocean Engineering **38**, pp. 699-711.

Rozhdestvensky, K. V. & Ryzhov, V. A. (2003). 'Aerohydrodynamics of flapping-wing propulsors'. Progress in aerospace sciences **39**, pp. 585-633.

Read, D. A., Hover, F. S. & Triantafyllou, M. S. (2003). 'Forces on oscillating foils for propulsion and maneuvering'. J. Fluids and Structures **17**, pp. 163-183.

Saffman, P.G. (1992). Vortex Dynamics. Cambridge University Press.

Schouveiler, L., Hover, F. S. & Triantafyllou, M. S. (2005). 'Performance of flapping foil propulsion'. J. Fluids and Structures **20**, pp. 949-959.

Shyy, W., Lian, Y., Tang, J., Viieru, D. & Liu, H. 'Aerodynamics of Low Reynolds Number Flyers'. Cambridge Aerospace Series.

Shyy, W., Aonoa, H., Chimakurthia, S.K., Trizilaa, P., Kanga, C.-K., Cesnika, C. E. S. & Liub, H. (2010). 'Recent progress in flapping wing aerodynamics and aeroelasticity. Progress in aerospace sciences.

Sparenberg, J. A. (2002). 'Survey of the mathematical theory of fish locomotion'. J. Engineering Mathematics **44**, pp. 395-448.

Taylor, G. K, Triantafyllou, M. S & Tropea, C. (2010). Animal Locomotion. Springer Verlag.

Triantafyllou, M. S., Triantafyllou, G. S. & Gopalkrishnan R. (1991). 'Wake mechanics for thrust generation in oscillating foils'. Phys. Fluids, **A 3**(12).

Triantafyllou, M. S., Triantafyllou, G. S. & Grosenbaugh M. A. (1993). 'Optimal thrust development in oscillating foils with application to fish propulsion'. Journal of Fluids and Structures 7, pp. 205-224.

Triantafyllou, M. S., Triantafyllou, G. S. & Yue, D. K. P. (2000). 'Hydrodynamics of fishlike swimming'. Annual Rev. of Fluid Mech.

Triantafyllou, M. S., Techet, A. H. & Hover, F. S. (2004). 'Review of Experimental Work in Biomimetic Foils'. IEEE Journal of Oceanic Engineering **29**(3).

Yu, J., Hu, Y., Huo, J. & Wang, L. (2009). 'Dolphin-like propulsive mechanism based on an adjustable Scotch yoke'. Mechanism and Machine Theory **44**, pp. 603–614.

Wu, T. Y. (1971). 'Hydromechanics of swimming propulsion. Part 1. Swimming of a two-dimensional flexible plate at variable forward speeds in an inviscid fluid'. J. of Fluid Mechanics **46**, pp. 337–355.

Zhu, Q., Wolfgang, M. J., Yue, D. K. P. & Triantafyllou M. S. (2002). 'Three dimensional flow structures and vorticity control in fish-like swimming'. J. of Fluid Mechanics **468**, pp. 1-28.